ISSN 2347 - 3983
Volume 8. No. 10, October 2020
International Journal of Emerging Trends in Engineering Research
Available Online at http://www.warse.org/IJETER/static/pdf/file/ijeter1248102020.pdf
https://doi.org/10.30534/ijeter/2020/1248102020

Mathematical Modeling of a Star Sensor

Alipbayev K.[1], Saurova K.[2], Demesinova S.[3], Sydykov R.[4], Balbayev G.[5]
[5]Gylym Ordasy, Almaty, Kazakhstan, e-mail: gani_b@mail.ru
[1,2,5]Almaty University of Power Engineering and Telecommunications, Kazakhstan, e-mail: gani_b@mail.ru
[3,4]Al-Farabi Kazakh National University, Kazakhstan

ABSTRACT

This article describes an introduction to star sensors as one of the spacecraft orientation tools and an analysis of mathematical and software modeling of the star sensor. And also in this article mathematical calculations and modeling of the star sensor are presented. All calculations are based on existing systems and a star sensor, in addition, a brief software presentation of the system, algorithms of the software product are presented.

Key words: (SC) spacecraft, star sensor, mathematical modeling of the star sensor, orientation of the star sensor, motion coordinates of the star sensor

1.INTRODUCTION

After the conquest of outer space by the first man, humanity began active space exploration, thus there were problems with the orientation and stabilization of the spacecraft (SC). Orientation AS necessary for proper movement in orbit and the most efficient reception and transmission of information. Currently, there are two orientation systems: active and passive. The passive system includes gravitational, aerodynamic, and electromagnetic orientations. All of them do not require spacecraft power and are the most economical, but less accurate sensors. The active system includes gyroscopes, jet nozzles, flywheels, star and solar sensors, and so on. their operation requires the energy of the spacecraft, thus they are less economical, but more accurate. Among all orientation sensors, the star sensor is one of the most accurate and sophisticated instruments on the spacecraft.

Now the use of the star sensor in the modern space industry has become an integral part of the development of spacecraft. Mathematical and software modeling is used for development, as it will be possible to test the system for failures and failures, improve the system and minimize failures on a real device.

In the first half of the thesis, mathematical calculations and modeling of the star sensor will be presented. All calculations will be based on existing systems and the star sensor. In the second half, a brief program presentation of the system and algorithms of the software product will be presented.

The purpose of the article is to research and develop a mathematical and software simulation of a star sensor. Start of development of a domestic analog of this software product.

Relevance of the article. Software development for the star sensor is a very expensive sensor element and development in Kazakhstan can reduce the cost of manufacturing spacecraft and further enter the market as a competitive manufacturer.

After the beginning of the space age, engineers faced many new challenges and problems during the flight of the spacecraft. This number included the problem of chaotic movement around its axis. It is the orientation around its axis that directly affects the efficiency and accuracy of orbit movement and maneuver execution. This problem has been solved by a variety of orientation sensors, and the newest is the star sensor. The first use of this sensor occurs in the second half of the 80 - ies of the last century.

This new development was actively used in the United States (JPL), the Institute for Space Research of the USSR Academy of Sciences, France (SODERN), the German Democratic Republic (Karl Zeiss Jena) and Italy (Galileo).

The Astro star sensor and orientation system were installed at Mir station, and after working there successfully for 11 years, it was also used to sink the station into the ocean.

At the moment, there are more than ten foreign manufacturers of star sensors and software for them: Jena-Optronik, SODERN, Ball Aerospace, Goodrich, Galileo Avionica, Terma, etc. [1, 6,7,8].

Unfortunately, the Republic of Kazakhstan does not have domestic manufacturers of star sensors.

Star tracker (in foreign sources, " astrosensor ") is a device for determining the orientation of the spacecraft using the starry sky. The orientation of the star sensor in outer space occurs through a lens and detector that record images of the starry sky and compare them with stars from the star catalog. Usually a star sensor is based on a CCD (charge-coupled device), which consists of a set of light-sensitive photodiodes. The field of view of the lens can be calibrated from 10 to 25 degrees, and the mass of the sensor varies in the range of 2-5 kilograms. The sensitivity of the detector also depends on the model and customer requirements.

A lot of interference occurs when using a star sensor, including image flare and small particles getting into the sensor lens. To work out such interferences and failures, simulated conditions are produced for test models on the ground.

Figure 1: SODERN star sensor

2. STAR SENSOR WORKING PRINCIPLE

All parts of the star sensor can be divided into:
- optical components (lens, etc.);
- photosensitive components (photodetector);
- electronic components (photodetector electronics, data processing electronics, memory).

The star sensor determines its location in the inertial coordinate system by observing the starry sky in the visible wavelength range. The sensor receives an image of the visible starry sky using the lens built into the sensor. In the resulting image, images of stars are identified, for which coordinates are determined on the matrix radiation receiver. The characteristics of stars in the frame are compared with the catalog of stars stored in the memory of the star sensor, for which the celestial coordinates in the Equatorial coordinate system are known. The result of the comparison is the identification of the starry sky from the catalog with the images of stars in the image. These stars are used to calculate the orientation of the stellar sensor relative to the inertial coordinate system associated with fixed stars. This orientation detection action is repeated periodically. The maximum repetition rate of the orientation detection action is 10 Hz. Calibration of the star tracker shall be held as degradation of the photosensitive CCD-matrix. Repeated calibrations depend on the radiation situation. Also in the sensor is a thermoelectric refrigerator to increase the temperature of the photodetector.

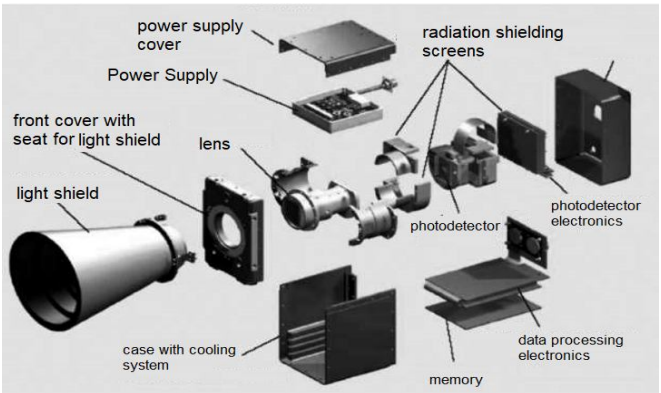

Figure 2: Main elements of the star sensor

First, let's look at the coordinate systems of the star sensor movement. To do this, we introduce two right Cartesian coordinate systems with the zero-point O in the center of the celestial sphere [1].

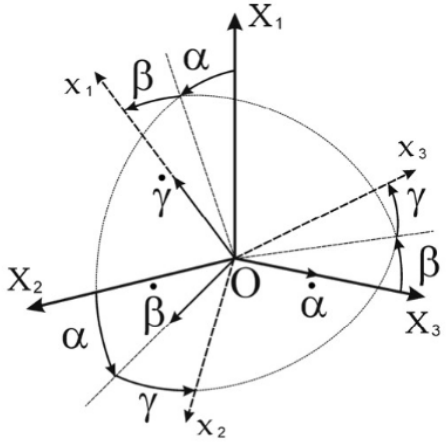

Figure 3: Relativity of the inertial and mobile coordinate systems.

$OX_1X_2X_3$ — integral (basic) coordinate system. The first axis lies on the plane of the celestial equator and looks at the point of the vernal equinox; the third axis lies on the axis of rotation of the Earth; and the second axis is the complement of the right three.

$Ox_1x_2x_3$ — a mobile but spacecraft-related coordinate system whose axes are the axes of the satellite where the star sensor is installed. It is assumed that the optical sensor coincides with Ox_1, a plane parallel with the photo editor Ox_2x_3.

The orientation of the mobile system can be written in matrix form:

$$X = Ax = \begin{vmatrix} a_{11} & a_{12} & a_{13} \\ a_{21} & a_{22} & a_{23} \\ a_{31} & a_{32} & a_{33} \end{vmatrix} \cdot x, \qquad (1)$$

Where:

$$a_{11} = \cos a \cos b,$$
$$a_{12} = \sin a \sin y - \cos a \sin b \cos y,$$
$$a_{13} = \sin a \cos y + \cos a \sin b \sin y,$$
$$a_{21} = \sin b,$$
$$a_{22} = \cos b \cos y,$$
$$a_{23} = -\cos b \sin y,$$
$$a_{31} = -\sin a \cos b,$$
$$a_{32} = \cos a \sin y + \sin a \sin b \cos y,$$
$$a_{33} = \cos a \cos y - \sin a \sin b \sin y.$$

Equation of motion of the SPACECRAFT:

$$J\omega + \omega \times J\omega = M_0, \qquad (2)$$

where J is the inertia tensor calculated on the main axes.
ω is the vector of absolute angular velocity.

M_0-Vector of the total moment of external forces.
Dynamic equations of kinematic Poisson relations:

$$\tau_i = \omega \times \tau_i, \quad (3)$$

Where τ_i is the orthopedic orientation of the moving coordinate systems.
When integrating the displacements, ((2), (3)) zero moment and axisymmetric spacecraft are used, perform regular precession with known constraints. For this purpose, the mathematical modeling of the orbital and relative motion under the influencing, restoring and controlling moments of various types of nature has been implemented [2].

Here are some of them:
- gravitational moment:

$$M_0^{gm} = \frac{3\mu_g}{r^3} E \times JE,$$

where μ is the gravitational parameter of the attracting center;
r is the distance from the attracting center to the SC center of mass.
E is the unit vector of the local vertical.
- magnetic moment:

$$M_0^{magn} = m \times B$$

where m is the vector of the total magnetic moment of the carrier.
B is the induction vector of the Earth's magnetic field.
- the control moment, creating the flywheels:

$$M_0^{\max} = -\mathrm{H} - \omega \times \mathrm{H}$$

where H is the angular momentum vector created by the flywheels.

In the numerical integration of motion, the vector equation (2) is projected on the axis of the moving coordinate system. The vectors m and H are naturally written in the moving system and require a transition to the linked axes. Let's calculate these vectors using the elements of the theory of orbital motion.

Let us take the orbital coordinate system of the spacecraft $OY_1Y_2Y_3$. The first axis is directed to the radius vector of the orbital position of the spacecraft, the second axis is located on the orbital plane, and the third axis complements the right orthogonal system.

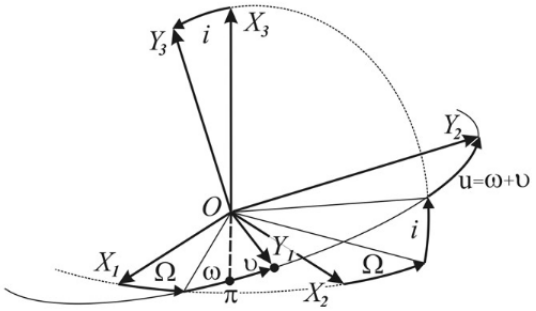

Figure 4: Orientation of the spacecraft coordinate system relative to the inertial one.

The ascending node longitude and inclination angles determine the position of the orbital plane. The eccentricity of the orbit (e) determines its shape, and the parameter of the orbit (p) determines its size. The angle of the periapsis argument (the angle between the line of nodes and the direction to the periapsis of the orbit) specifies the position of the orbit in the spacecraft plane. The moment of time when the spacecraft passes through the periapsis for the first time is considered known.

Getting $OX_1X_2X_3$ from $OY_1Y_2Y_3$ occurs after 3 consecutive turns. The first rotation is by the angle of the ascending node around the third inertial axis, the second turning on the inclination angle of the new position of the first inertial axis, the third rotation angle argument of latitude around the new third inertial axis. The relationship between two coordinate systems can be described in matrix form:

$$X = CY, \quad (4)$$

Where

$$C = \begin{pmatrix} \cos\Omega\cos u - \sin\Omega\sin u\cos i & -\cos\Omega\sin u - \sin\Omega\cos u\cos i & \sin\Omega\sin i \\ \sin\Omega\cos u + \cos\Omega\sin u\cos i & -\sin\Omega\sin u + \cos\Omega\cos u\cos i & -\cos\Omega\sin i \\ \sin u\sin i & \cos u\sin i & \cos i \end{pmatrix}$$

The position of the SPACECRAFT in orbit (the distance from the attracting center to the center of mass of the SPACECRAFT and the gravitational parameter of the attracting center) can be determined using the following equations:

$$t - \tau_\pi = \frac{a^{3/2}}{\mu^{1/2}}(E - e\sin E), \quad (5)$$

$$tg\frac{\vartheta}{2} = \sqrt{\frac{1+e}{1-e}}\, tg\frac{E}{2}, \quad (6)$$

where $a = p/(1 - e^2)$ is the semimajor axis of the orbit;
E is an eccentric anomaly.
Expression (5) describes the relationship between time and the position of the spacecraft in orbit, expressed in terms of an eccentric anomaly, and expression (6) – the relationship between eccentric and true anomalies.

Let's use expression (4) to write vectors E and B in the inertial coordinate system. The vector of the true vertical in the system $OY_1Y_2Y_3$ can be written as

$$E^{OY} = (1\ 0\ 0)^T$$

and the geomagnetic field induction vector has the form:

$$B^{OY} = B_0 \begin{pmatrix} -2\sin u \sin i \\ \cos u \sin i \\ \cos i \end{pmatrix}$$

The vector E in projections on the axis $OX_1X_2X_3$ can be written as:

$$E^{OX} = \begin{pmatrix} \cos\Omega\cos u - \sin\Omega\sin u\cos i \\ \sin\Omega\cos u + \cos\Omega\sin u\cos i \\ \sin u\sin i \end{pmatrix}$$

Numerical integration of the equations of motion (2) and (3) with the given initial conditions, system parameters, and elements of the spacecraft orbit allows us to determine the matrix of guiding cosines (the current orientation of the sensor relative to the inertial system) at each time. In accordance with the user-defined field of view of the camera, the "observed" part of the space is determined. The spherical coordinates of stars (α, δ) are converted into Cartesian coordinates of the inertial system $OX_1X_2X_3$, which are translated into a mobile system $(Ox_1x_2x_3)$ using a well-known matrix of guiding cosines. The location of stars in the mobile coordinate system is converted to spherical coordinates (φ, θ), which determines the direction of the vector to the star.

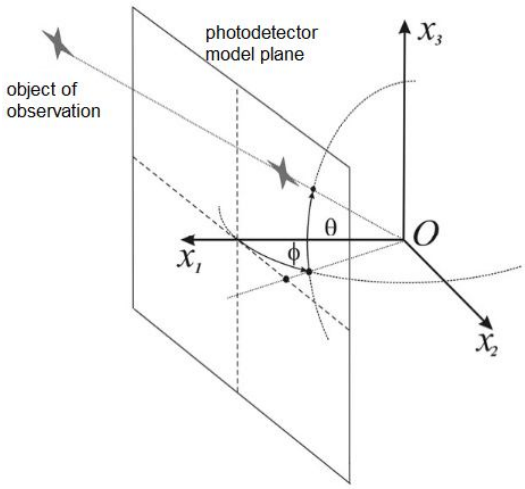

Figure 5: Finding the direction of the vector to the star in the mobile coordinate system.

Using a perspective projection, the observed stars from the spherical system (φ, θ) move to a rectangular coordinate system associated with the model plane of the photodetector (Fig. 5) and will be displayed on the monitor. The brightness and size of the displayed stars are functions of the magnitude of the star; the number of stars displayed is a configurable parameter.

You can also implement the function of displaying background objects: illuminating a part of space, finding and displaying objects that are stationary (dust on the lens) and mobile (space debris) relative to the detector plane.

As a test star sensor, let's take the HYDRA-CP model from SODERN [3].

Table 1 - characteristics of THE Hydra-CP star sensor

The name of the sensor	HAS-2 (CMOS)
Pixel sizes	18 mcm
Matrix size	18.4 x 18.4 mm
Permission	1024x1024 pixels
Built-in lens	18.5 mm f2.6 H40^0
Max. Frame rate	30 frames / sec.
Connection interface	USB

The image transmitted by the simulator is “captured " by the camera. Frame-by-frame analysis of the obtained video images is performed in a rectangular coordinate system associated with the detector plane (Fig. 6).

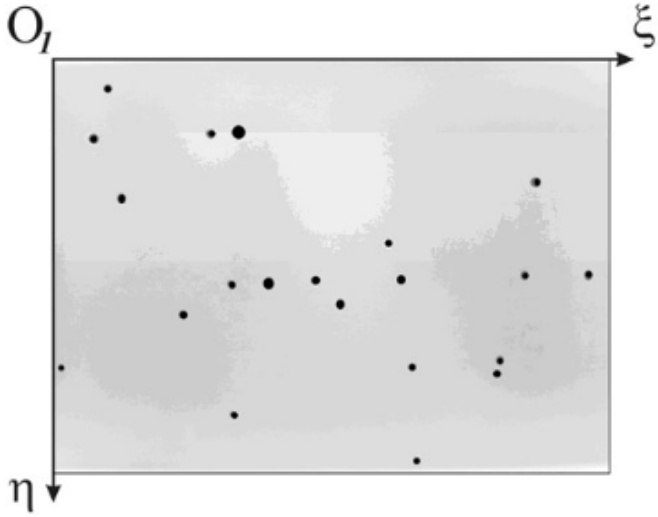

Figure 6: The coordinate system associated with the detector plane.

The problem of star recognition is solved in an idealized setting. The simulated images of the starry sky do not contain objects of complex configuration. In particular, tracks whose nature is significant angular velocities of the camera and noise caused by the passage of protons through the CCD at a large angle to its optical axis are not displayed. As noted earlier, images transmitted to the camera contain only point objects (stars and interference) and noise that mimics third-party inhomogeneous illumination.

The procedure for recognizing the image of the starry sky is carried out in several stages. At the beginning, noise highlights are filtered by dividing the image into subdomains

and subtracting the average intensity values in the corresponding area from the current intensity of each pixel. This partitioning is necessary to deal with non-uniform highlights. After that, the filtered image is scanned, and the signal maxima local to the subdomains are determined. The integral signal intensity in the vicinity of the detected maxima is compared with the current noise value according to the specified detection criterion. When the criterion is met, the object is considered detected, and its center of mass is calculated in the coordinate system associated with the detector plane:

$$\xi_c = \frac{\sum \xi_i I_i}{\sum I_i}, \eta_c = \frac{\sum \eta_i I_i}{\sum I_i}$$

where (ξ, n) are the coordinates of the image pixels that fall within the localization area of the point signal;

I-corresponding intensities (figure 7)

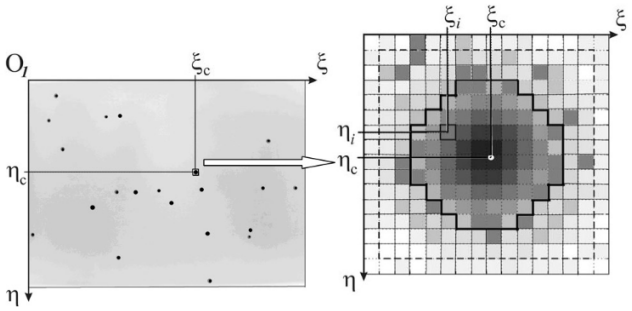

Figure 7: Calculating the star and determining the center of mass.

The procedure for recognizing calibration grid nodes is slightly different from recognizing simulated images of the starry sky. In this case, you need to find a large number of stars (from 100 to 400), without missing any. At the same time, it is necessary to establish the locations of all stars relative to the Central point of the grid in order to further establish an unambiguous correspondence between the simulated and recognized stars.

Recognition begins with a Central point that is slightly different in size from the rest of the stars and serves as a good sign for identifying it. After that, a priori information about the grid structure is used, which allows you to predict the position of images of neighboring nodes based on previously detected ones. This method simplifies the search and detection of stars by reducing it to a forecast-confirmation-correction algorithm, and also allows you to automatically get the desired match between simulated and detected stars.

You should pay attention to the problem of localizing a point object – the selected area of the image (a group of pixels), which is taken into account when calculating the center of mass. In this article, we used a rectangular area in which the source image is inscribed. All pixels of the image that fell into this area were taken into account when calculating its coordinates. However, this method has significant disadvantages, since it does not take into account the actual shape of the image. An increase in accuracy in determining the coordinates of the center of mass can be achieved by solving this problem of finding the image contour. The next level of accuracy can be obtained by using the distribution functions of the observed signal of a point object. In other words, the localized signal is interpolated on an analytical function (Fig. 8), whose distribution parameters are estimated at the stage of device calibration at different angles of the source orientation relative to the optical axis.

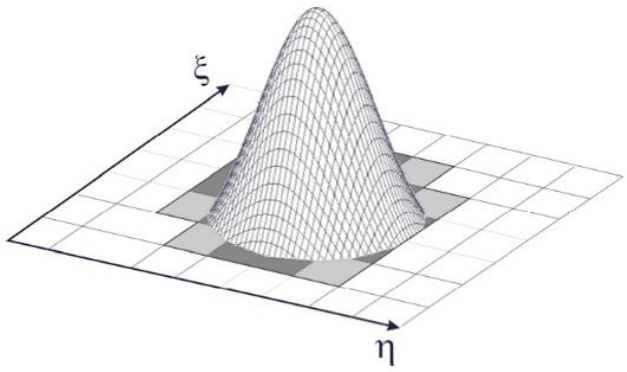

Figure 8: Three-dimensional distribution function of the received signal.

In this case, various optical effects can be taken into account, such as distortion in the extreme areas of the image and, as a result, the accuracy of the device is increased.

After performing star recognition and determining the actual angular distances between them using previously prepared calibration functions, they are determined by comparing the obtained configurations with the configurations presented in the star catalog.

The problem of detecting stars, along with the problem of recognition, is the main factor that determines the quality of the device as a whole. This is the most resource-intensive operation, and if the correct solution of the identification problem in General determines the accuracy, then the system speed directly depends on the methods of solving the identification problem [4].

One of the main ideas that is basic in the implementation of many identification algorithms is that stars from the catalog are represented as vertices of an undirected graph G1, whose edge weight is equal to the angular distance between the stars. Objects found after analyzing the captured frame are also represented as an undirected graph G2. The main task is to implement fast methods for finding a subgraph from G that is isomorphic to G2.

Another group of identification algorithms includes the so-called grid algorithms, the main idea of which is that each star is associated with a bit matrix (or pattern). The value of the matrix field is 1 if it includes a star adjacent to the selected one. Otherwise, the field value is 0.to determine star configurations, a bitwise comparison of the matrices constructed for the analyzed image with the corresponding templates from the catalog is used.

All these algorithms are of the "Lost In Space" type (hereinafter referred to as LIS) and are characterized by the fact that their implementation does not require any a priori

information about the current orientation and angular velocity of the camera.

If there is a priori data about the sensor movement obtained from third-party devices or pre-calculated using LIS algorithms, the position of stars in the detector system can be predicted with high accuracy. In this case, the recognition and detection tasks are reduced to the maintenance task performed according to the forecast-correction scheme, which significantly increases the performance of the system as a whole.

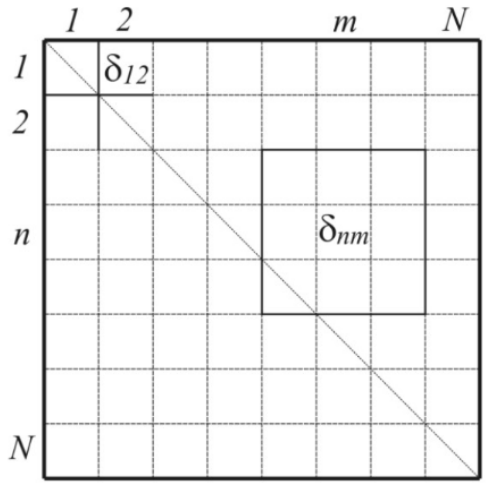

Figure 9: Diagram of the angular distance table

In this work, an algorithm optimized for search speed was chosen. The catalog size is limited to the N brightest stars. Each star is assigned a unique number. A table of size N x N is created with the values of angular distances between stars with corresponding numbers in its cells (Fig. 9). Using the built table, you can quickly access the distance by star numbers [5].

After that, a list is created (figure 10), each row of which contains information about the numbers of stars and the corresponding angular distance between them. The list is limited according to the angle of view of the sensor used and ordered in ascending order of distances.

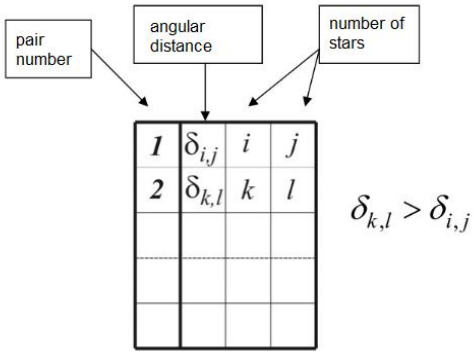

Figure 10: List of distances between them with comparison by star catalog.

The algorithm for determining observed stars uses the 5 brightest objects in the image. One object is selected, and the angular distances to the remaining four are calculated. for each of them, matching pairs are found in the distance list. Next, a list of 5 stars is formed, for which the distance from the first to the other four is in the range $\delta \pm \varepsilon$, where ε is the accuracy of the sensor in determining the angular distance. For each entry in the list, all distances between stars are determined (using the distance table), and their correspondence to the distances in the image is checked. If at least one distance does not match, we consider the following entry. The scheme of the identification algorithm is shown in Fig. 11.

If there are "phantoms" (objects that are not present in the catalog) among the 5 selected stars in the image, then the list will not contain any correct configuration. In this case, the star identification procedure is repeated with a different set of stars.

Using this algorithm, the detection was carried out when displaying 1500 objects, while information was present only about three hundred, that is, the proposed method successfully bypasses the problem of the presence of dim stars and "phantom" objects in images.

The problem of optimizing the search speed in the presence of "phantom" objects, as well as the problems of detailed analysis of the algorithm in comparison with existing approaches may be the subject of future research.

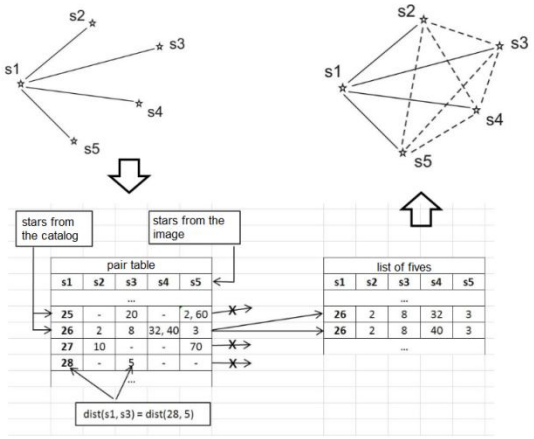

Figure 11: Diagram of the algorithm for determining stars.

You can also note the object tracking algorithm. In this case, a priori information about the current orientation of the camera and its angular velocity was transmitted from the simulator to the frame processing module, the position of the corresponding stars in the detector coordinate system was predicted, the selected image regions were recognized, their presence was confirmed, the positions of the image centers of mass were corrected, and the procedure for comparing the detected configuration with the forecast one was performed. This approach significantly increased the speed of the system as a whole.

For fige. 12 an example of a recognized image and identified objects is presented. Among all the detected point objects, the nine brightest ones are highlighted (double border). The identification was carried out for 5 objects.

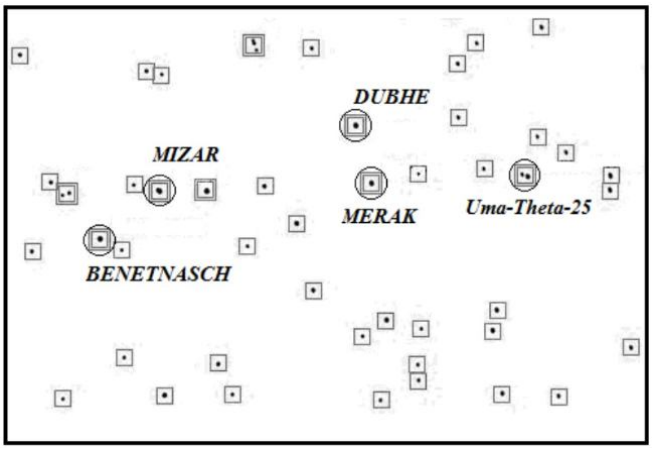

Figure 12: Determining the image of stars.

Determining the current orientation of the SPACECRAFT is reduced to solving an optimization problem of the form:

$$\min_{\{a_{jk}\}} \sum_{i=1}^{n} \|X_i - Ax_i\|$$

where n is a list of certain stars;
X-coordinates of the i-th star in the inertial coordinate system.
x – corresponding coordinates in the mobile coordinate system. In this case, the elements of the matrix of guide cosines a j k must satisfy the orthogonality conditions.
In this case, we will consider a method for determining the current matrix of guiding cosines, the essence of which is as follows.

Let S_{ji} be the coordinates of 3 stars in the detector coordinate system (j = 1...3 is the index of the corresponding point, i = 1...3 is the coordinate projected on the corresponding axis), and S_{ji} be the corresponding coordinates in the inertial system. The elements of the matrix of guiding cosines are determined in the course of solving equations of the form:

$$\begin{pmatrix} S_{j1} \\ S_{j2} \\ S_{j3} \end{pmatrix} = \begin{Vmatrix} a_{11} & a_{12} & a_{13} \\ a_{21} & a_{22} & a_{23} \\ a_{31} & a_{32} & a_{33} \end{Vmatrix} \times \begin{pmatrix} s_{j1} \\ s_{j2} \\ s_{j3} \end{pmatrix}$$

The following equality is obvious

$$S_{ji} = \sum_{k=1}^{3} a_{jk} s_{jk},$$

which after the introduction of the auxiliary matrix:

$$D = \begin{vmatrix} s_{11} & s_{12} & s_{13} \\ s_{21} & s_{22} & s_{23} \\ s_{31} & s_{32} & s_{33} \end{vmatrix}$$

grouped into the following 3 algebraic systems

$$\begin{pmatrix} S_{j1} \\ S_{j2} \\ S_{j3} \end{pmatrix} = D \begin{pmatrix} a_{i1} \\ a_{i2} \\ a_{i3} \end{pmatrix}$$

Whence it follows that

$$\begin{pmatrix} a_{i1} \\ a_{i2} \\ a_{i3} \end{pmatrix} = D^{-1} \begin{pmatrix} S_{1i} \\ S_{2i} \\ S_{3i} \end{pmatrix}$$

Next, we perform several calculations (for different triples), average the result, and perform orthogonalization of the matrix of guiding cosines.
Using two known camera orientations A(k) and A(k+1) separated by an interval t, the angular velocity of the SPACECRAFT rotation can be found by solving the Poisson equation:

$$\frac{dA}{dt} = \Omega A, \Omega = \begin{pmatrix} 0 & -\omega_3 & \omega_2 \\ \omega_3 & 0 & -\omega_1 \\ -\omega_2 & \omega_1 & 0 \end{pmatrix}$$

where ω is the projection of the absolute angular velocity on the axis of the inertial coordinate system.

In that case

$$\Omega = \frac{dA}{dt} A^{-1} \approx \frac{A_{k+1} - A_k}{\Delta t} \left(\frac{A_{k+1} + A_k}{2} \right). [2]$$

REFERENCES

1. Moldabekov, M., Akhmedov, D., Yelubayev, S., Ten, V., Albazarov, B., Shamro, A., Alipbayev, K., Bopeyev, T., Sukhenko, A. Features of design and development of the optical head of star tracker. Proceedings of SPIE - The International Society for Optical EngineeringVolume 9241, 2014, Номер статьи 924122Sensors, Systems, and Next-Generation Satellites XVIII; Amsterdam; Netherlands; 22 September 2014 до 25 September 2014.
2. Akhmedov, D., Yelubayev, S., Ten, V., Bopeyev, T., Alipbayev, K., Sukhenko, A. Software and mathematical support of Kazakhstani star tracker . Proceedings of SPIE - The International Society for Optical EngineeringVolume 10000, 2016, Номер статьи 100001SSensors, Systems, and Next-Generation Satellites XX; Edinburgh; United Kingdom; 26 September 2016 до 28 September 2016.
3. Ruban S. V. Development of algorithmic support for a multi-collimator rotary stand for testing stellar orientation sensors. // MEI, Moscow, 2008-31 p.
4. A. A. Degtyarev, S. S. Tkachev, D. A. Mylnikov, Laboratory equipment for small satellite stars tracker

prototype elaboration. [http://library.keldysh.ru/preprint.asp?id=2010-67]
4. NOIH2SM1000A. HAS2 Image Sensor [http://onsemi.com].
5. R. R. Nazirov. All-Russian scientific and technical conference modern problems of determining the orientation and navigation of spacecraft. Astroorientation and navigation devices for spacecraft. Television systems of the Phobos-grunt project. Methods and means of ground testing of optoelectronic devices. Multi-zone survey systems for remote sensing. Collection of works. – Russia, Tarusa, 2008 – 580 c.
6. Nasarudin Ismail, Mohd Murtadha Mohamad, Mohamad Aizi Salamat, Simulation and Visualization of Acoustic Underwater Sensor Networks using Aqua-Sim and Aqua-3D An Evaluation. International Journal of Advanced Trends in Computer Science and Engineering. Volume 8, No.3, 2019, pp. 943-948.
7. Emmanuel Trinidad, Lawrence Materum, "Juxtaposition of Extant TV White Space Technologies for Long-RangeOpportunistic Wireless Communications", *International Journal of Emerging Trends in Engineering Research.* Volume 7, No. 8, 2019, pp. 209-215.
8. Kihong Shin, "On the Selection of Sensor Locations for the Fictitious FRF based Fault Detection Method", *International Journal of Emerging Trends in Engineering Research,* Volume 7, No. 11, 2019, pp. 569-575.